

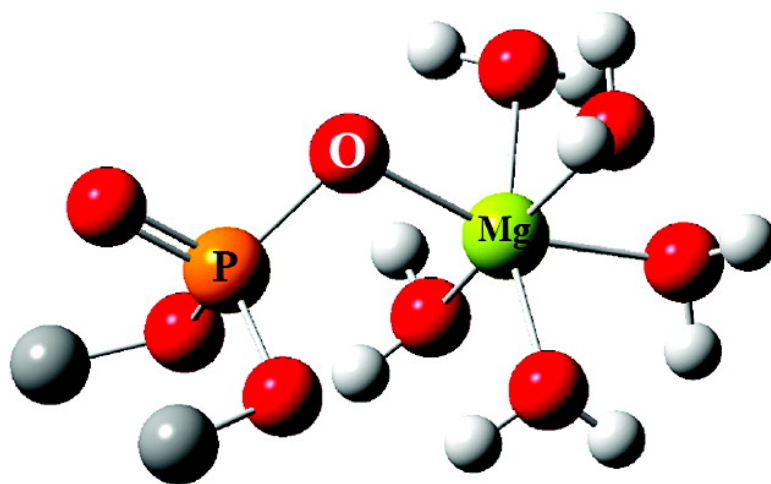
Communication

## Detection of Innersphere Interactions between Magnesium Hydrate and the Phosphate Backbone of the HDV Ribozyme Using Raman Crystallography

Bo Gong, Yuanyuan Chen, Eric L. Christian, Jui-Hui Chen, Elaine Chase, Durga M. Chadalavada, Rieko Yajima, Barbara L. Golden, Philip C. Bevilacqua, and Paul R. Carey

*J. Am. Chem. Soc.*, **2008**, 130 (30), 9670-9672 • DOI: 10.1021/ja801861s • Publication Date (Web): 01 July 2008

Downloaded from <http://pubs.acs.org> on February 8, 2009



### More About This Article

Additional resources and features associated with this article are available within the HTML version:

- Supporting Information
- Links to the 1 articles that cite this article, as of the time of this article download
- Access to high resolution figures
- Links to articles and content related to this article
- Copyright permission to reproduce figures and/or text from this article

[View the Full Text HTML](#)



**ACS Publications**  
High quality. High impact.

## Detection of Innersphere Interactions between Magnesium Hydrate and the Phosphate Backbone of the HDV Ribozyme Using Raman Crystallography

Bo Gong,<sup>†</sup> Yuanyuan Chen,<sup>†</sup> Eric L. Christian,<sup>†</sup> Jui-Hui Chen,<sup>‡</sup> Elaine Chase,<sup>‡</sup>  
Durga M. Chandalavada,<sup>§</sup> Rieko Yajima,<sup>§</sup> Barbara L. Golden,<sup>\*,‡</sup> Philip C. Bevilacqua,<sup>\*,§</sup> and  
Paul R. Carey<sup>\*,†</sup>

*Department of Biochemistry, Case Western Reserve University, 10900 Euclid Avenue, Cleveland, Ohio 44106,  
Department of Biochemistry, Purdue University, 175 South University Street, West Lafayette, Indiana 47907, and  
Department of Chemistry, The Pennsylvania State University, 104 Chemistry Building,  
University Park, Pennsylvania 16802*

Received March 17, 2008; E-mail: paul.carey@case.edu; pcb@chem.psu.edu; barbgolden@purdue.edu

Metal cation binding lies at the heart of much of RNA chemistry and is crucial for RNA folding and ribozyme catalysis.<sup>1,2</sup> Because RNA is a polyanion, metal–RNA interactions are both plentiful and complex. Current methods of characterization have limitations in their abilities to directly detect the type of metal–RNA interactions and their ligands. For example, while NMR spectroscopy can be used to look at binding and structures of outersphere complexes to RNA via  $\text{Co}(\text{NH}_3)_6^{3+}$ , evidence for innersphere sites is often less direct.<sup>3</sup> Phosphorothioate activity–rescue experiments, although providing a number of notable successes,<sup>4</sup> still require modification of the RNA and do not report on the coordination number of the metal ion.

A Raman microscope and Raman difference spectroscopy provide a complementary method to study the interactions of metal ions with complex RNAs. Here, we detect the vibrational signatures of RNA-bound magnesium hydrate in crystals of hepatitis delta virus (HDV) ribozyme and follow the effects of magnesium hydrate binding to the nonbridging phosphate oxygens in the phosphodiester backbone. Raman provides both a direct spectroscopic probe of innersphere contacts and characterization of the chemical nature of the complex. The Raman experimental approach used to elicit the data is described in Gong et al.,<sup>5</sup> and the HDV ribozyme was selected for our initial studies on magnesium binding on the basis of extensive biochemical and structural data.<sup>6,7</sup>

The HDV ribozyme is an ~85 nt RNA that functions in the life cycle of the human HDV.<sup>8</sup> We developed a two-piece 71 nt construct for crystallographic studies in which the catalytic 2'-OH on the U-1 group was modified to prevent the cleavage reaction occurring in the crystals in the presence of  $\text{Mg}^{2+}$ .<sup>5</sup> The overall tertiary structure of HDV is shown in Figure 1, along with the metal binding sites. Herein, we demonstrate that in the HDV ribozyme crystals<sup>9</sup> there is a correlation between the Raman intensity of the signature peaks for innersphere magnesium hydrate (specifically Mg penta- and tetrahydrate) and the intensity of the  $\text{PO}_2^-$  symmetric stretch perturbed by magnesium binding, supporting a direct observation of  $\text{PO}_2^- \cdots \text{Mg}^{2+}(\text{H}_2\text{O})_x$  innersphere complexes (penta-hydrate,  $x = 5$ ; tetrahydrate,  $x = 4$ ).

The properties of  $\text{Mg}^{2+}$  in aqueous solution, including its Raman and infrared active modes, have been well-characterized. The magnesium cation in solution exists as the stable hexahydrate<sup>1</sup> that has a totally symmetric stretching frequency at  $360 \text{ cm}^{-1}$ ,<sup>10</sup> which shifts to  $341 \text{ cm}^{-1}$  when the  $\text{Mg}^{2+}$  is surrounded by  $\text{D}_2\text{O}$  or  $\text{H}_2^{18}\text{O}$  (confirmed in Figure S1, Supporting Information).

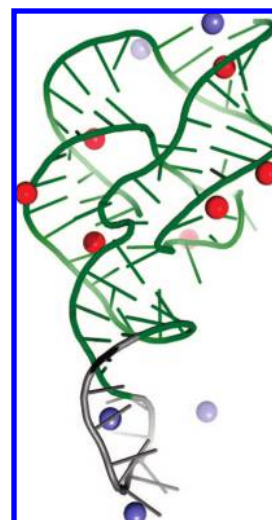


**Figure 1.** Crystal structure of the HDV ribozyme. The RNA is drawn with a coil representing the phosphodiester backbone and rods illustrating the position of the nucleotide bases. The native ribozyme sequence is green, and the non-native sequence introduced to bind the U1A protein is gray. Magnesium ions bound by the ribozyme core are red (see Table S1 and accompanying discussion), while those bound to non-native sequences or sequences not present in the RNA used in the current study are blue. Coordinates are from pdb entry 1cx0.

Using a Raman microscope, we recorded the Raman spectra of HDV ribozyme crystals in the presence of 0–40 mM  $\text{Mg}^{2+}$  in buffers containing 50–150 mM  $\text{Na}^+$ , which was present to maintain folding under low  $\text{Mg}^{2+}$  conditions. To obtain spectra in 0 mM  $\text{Mg}^{2+}$  conditions, magnesium was removed from the crystals by introducing 50 mM  $\text{Na}_2\text{EDTA}$  (raising  $[\text{Na}^+]$  to 150 mM) into the liquor surrounding the crystal. This process was repeated five times during 20 h to ensure that all bound  $\text{Mg}^{2+}$  ions have been removed from the crystal. Partial Raman difference spectra [HDV + 20 mM  $\text{Mg}^{2+}$ ] minus [HDV no  $\text{Mg}^{2+}$ ] are shown in Figure 2.<sup>11</sup> Signature features are observed near  $1100\text{--}1120$  and  $322 \text{ cm}^{-1}$  and can be attributed to phosphate groups on the RNA and to RNA-bound magnesium hydrate ions, respectively.

The differential feature near  $1100 \text{ cm}^{-1}$  is due to the symmetric stretch of  $\text{PO}_2^-$ .<sup>12</sup> In the parent Raman spectrum of the HDV ribozyme crystal in 20 mM  $\text{Mg}^{2+}$ , all 71 backbone  $-\text{PO}_2^-$ s in our construct contribute to a large peak near  $1100 \text{ cm}^{-1}$  (see Figure 4 in Gong et al.<sup>5</sup>). In the presence of  $\text{Mg}^{2+}$ , a fraction of the Raman signal for  $\text{PO}_2^-$  symmetric stretch ( $\nu\text{PO}_2^-$ ) moves to  $1117 \text{ cm}^{-1}$ . The positive node in the differential (Figure 2) arises from

<sup>†</sup> Case Western Reserve University.

<sup>‡</sup> Purdue University.

<sup>§</sup> The Pennsylvania State University.

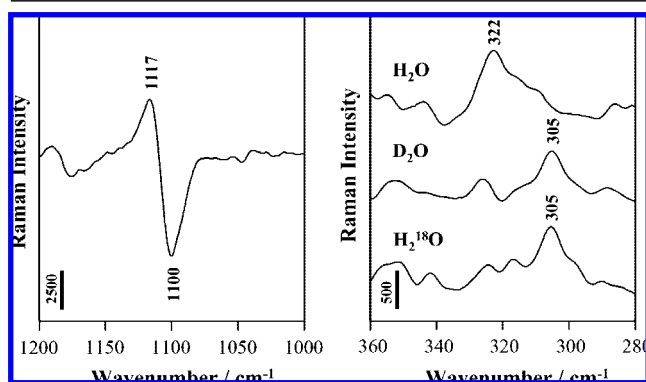


**Figure 2.** Raman difference spectra of HDV crystals [HDV + 20 mM  $\text{Mg}^{2+}$ ] minus [HDV no  $\text{Mg}^{2+}$ ], pH 6.0, 647 nm, 60 mW laser excitation;  $10 \times 10$  s data accumulation. Vertical bar represents photon events. Overall experimental details are given in Gong et al.<sup>5</sup> Left: partial Raman spectrum showing  $\text{PO}_2^-$  symmetric stretch of phosphate groups bound innersphere to  $\text{Mg}^{2+}$  at  $1117 \text{ cm}^{-1}$ ; the negative differential at  $1100 \text{ cm}^{-1}$  is due to phosphate symmetric stretch of metal-free groups. Right: Raman signatures of Mg hydrate (pentahydrate and tetrahydrate are both possible) bound innersphere to  $\text{PO}_2^-$  oxygen.

magnesium-bound phosphate groups that form a new vibrational mode upshifted by  $\sim 17 \text{ cm}^{-1}$  due to changes in vibrational coupling between the  $\text{PO}_2^-$  symmetric stretch and the adjacent C–O–P motions,<sup>13</sup> while the negative node at  $1100 \text{ cm}^{-1}$  results from the loss of a proportional fraction of the unbound or free  $\text{PO}_2^-$  symmetric stretch.

The second feature of note in the Raman difference spectra is the low intensity, but entirely reproducible, band near  $322 \text{ cm}^{-1}$ , which shifts to  $305 \text{ cm}^{-1}$  in  $\text{D}_2\text{O}$  or  $\text{H}_2^{18}\text{O}$  (Figure 2). These isotope shifts identify the  $322 \text{ cm}^{-1}$  feature as a normal mode involving vibrational motions of the metal oxygen bonds ( $\nu\text{MO}$ ) within magnesium hydrate. The likely identity of the magnesium hydrate species giving rise to the  $322 \text{ cm}^{-1}$  band can be deduced from the work of Peleg<sup>14</sup> who analyzed the properties of magnesium nitrate hexahydrate in aqueous solution and in ionic melts using Raman spectroscopy. In dilute aqueous solution, he identified the symmetric stretch of magnesium hexahydrate at  $363 \text{ cm}^{-1}$ , but in ionic melts where there are less than six water molecules per  $\text{Mg}^{2+}$ , a band at  $322 \text{ cm}^{-1}$  replaced this feature. The latter band was assigned to a magnesium hydrate mode where one or more of the coordinating waters are replaced by innersphere contacts to the nitrate oxygen. The assignment of a Raman feature in the  $320\text{--}330 \text{ cm}^{-1}$  region to innersphere-coordinated magnesium hydrate is further supported by a more recent study of Pye and Rudolf in aqueous  $\text{MgSO}_4$ .<sup>10</sup> Taken together, the isotope shifts and the literature studies lead us to assign the  $322 \text{ cm}^{-1}$  Mg hydrate band seen in the HDV ribozyme (Figure 2) to a magnesium complex that is six-coordinate but in which at least one of the ligands is an innersphere contact with a ligand from the RNA. This conclusion is further supported by quantum mechanical calculations carried out using Gaussian and by predictions of isotope effects (Supporting Information).

Magnesium hexahydrate in solution has perfect octahedral symmetry and has a symmetric stretching  $A_{1g}$  mode near  $360 \text{ cm}^{-1}$ , which moves to near  $341 \text{ cm}^{-1}$  upon  $\text{D}_2\text{O}$  or  $\text{H}_2^{18}\text{O}$  substitution. This isotope shift is predicted by quantum mechanical calculations, although our calculations give  $317$  and  $300 \text{ cm}^{-1}$  for the water and isotopically substituted  $\text{Mg}^{2+}$  hexahydrate, respectively. One reason for the overshoot is that the calculations used only single  $\text{Mg}^{2+}$  hexahydrate molecules, and these values are expected to increase as additional solvation shells are added.<sup>10</sup> Calculations for the  $\text{Mg}^{2+}$  pentahydrate model complex displayed in Figure 3A show

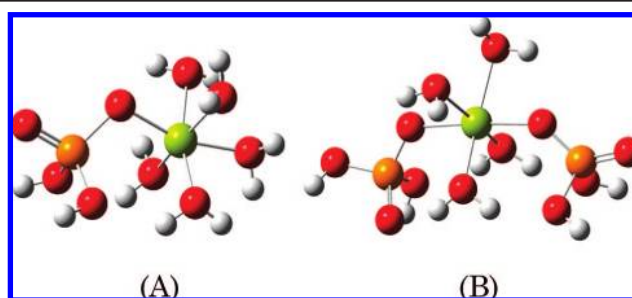


**Figure 3.** Models used in calculations. (A)  $\text{Mg}^{2+}$  pentahydrate– $\text{PO}_2^-$  complex using  $\text{H}_2\text{PO}_4^-$  as a model for the nonbridging  $-\text{PO}_2^-$  group at an RNA site. (B)  $\text{Mg}^{2+}$  tetrahydrate– $2\text{PO}_2^-$  complex, with the two  $-\text{PO}_2^-$  groups in the *trans* configuration. Colors of atoms:  $\text{Mg}^{2+}$  (yellow); oxygen (red); phosphorus (orange); hydrogen (gray). Calculations of analogues with dimethyl phosphate instead of  $\text{H}_2\text{PO}_4^-$  show similar  $\text{Mg}^{2+}$  hydrate vibrational features.

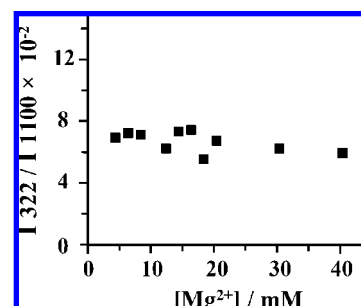


**Figure 4.** Ratio of intensities at  $322$  and  $1100$  (differential)  $\text{cm}^{-1}$  in the difference spectra as a function of  $\text{Mg}^{2+}$  concentration in liquor surrounding the HDV crystal.

that the  $\nu\text{MO}$  symmetric stretch is replaced by more complex motions involving the four equatorial waters and phosphate atom motions. This mode gives rise to a predicted feature at  $295 \text{ cm}^{-1}$ , which is a  $22 \text{ cm}^{-1}$  downshift as compared to the hexahydrate, consistent with the presence of pentahydrate in HDV. We also calculated two possible arrangements of magnesium tetrahydrate– $[\text{PO}_2^-]_2$  complex in vacuo, with two  $\text{PO}_2^-$  groups either at *trans* or *cis* positions in the octahedral template (Figure 3B). The results give values of  $279$  and  $290 \text{ cm}^{-1}$  for *cis* and *trans* magnesium tetrahydrate– $\text{PO}_2^-$  complexes, respectively, and the latter value is very close to the calculated value of magnesium pentahydrate– $\text{PO}_2^-$  complex. Thus, at the present level of our simple model compounds, it is difficult to use the calculations to confirm the exact values of the hydrate species in HDV. As such, both penta- $\text{Mg}^{2+}$ -hydrate, tetra- $\text{Mg}^{2+}$ -hydrate, or a mixture remain possibilities for the spectral features near  $322 \text{ cm}^{-1}$  in the HDV ribozyme.

Comparing the Raman signal for HDV in the presence and absence of  $\text{Mg}^{2+}$ , the appearance of the differential spectrum near  $1100 \text{ cm}^{-1}$  strongly suggests that  $-\text{PO}_2^-$  groups are involved in innersphere contacts. This notion is confirmed by  $\text{Mg}^{2+}$  titration experiments. As the HDV crystals are exposed to increasing concentrations of  $\text{Mg}^{2+}$  in the surrounding liquor, the intensities of both the “ $1100 \text{ cm}^{-1}$  negative differential” and the  $322 \text{ cm}^{-1}$  magnesium hydrate peak increase. As Figure 4 shows, there is a strong correlation between the two intensities, which strongly suggests that the appearance of the innersphere magnesium hydrate species is linked to the shift in the  $\text{PO}_2^-$  mode. Essentially identical spectra were obtained in the Raman spectra of aqueous solutions of the model compound dimethyl phosphate at molar concentrations of  $\text{Mg}^{2+}$  (Supporting Information, Figure S2). Dimethyl phosphate

should only be able to form 1:1 monodentate complexes with  $\text{Mg}^{2+}$ , thus demonstrating that a magnesium pentahydrate has a Raman peak near the  $322\text{ cm}^{-1}$ .

Using the  $1100\text{ cm}^{-1}$   $\text{PO}_2^-$  differential in Figure 2, we can estimate the number of phosphate groups per HDV molecule in innersphere complexes with  $\text{Mg}^{2+}(\text{H}_2\text{O})_x$ s from the ratio of the attenuated Raman signal in the presence of  $\text{Mg}^{2+}$  (the area of the negative limb at  $1100\text{ cm}^{-1}$  in the difference spectrum) to that of the  $1100\text{ cm}^{-1}$  peak in the parent spectrum of the HDV crystal in the absence of  $\text{Mg}^{2+}$ . At  $20\text{ mM Mg}^{2+}$ , this ratio is  $\sim 0.07$ , and since there are 71  $\text{PO}_2^-$ s in the HDV molecule, this suggests that there are on average  $\sim 5$  phosphates bound to  $\text{Mg}^{2+}(\text{H}_2\text{O})_x$ s under these conditions. While the above ratio changes as a function of  $\text{Mg}^{2+}$  concentration, a titration from 4 to  $40\text{ mM Mg}^{2+}$  suggests that the estimated value of  $\sim 5$  metal bound phosphates reflects a plateau in the dependence of the above ratio on  $\text{Mg}^{2+}$  concentration (Figures 4 and S3). This estimated number of phosphates bound is necessarily a lower limit because Raman signal may reflect partial occupancy of a larger number of sites, and because of the nature of the differential, some intensity may be lost when the two parent peaks are close together.

The presence of five innersphere  $-\text{PO}_2^- \cdots \text{Mg}^{2+}$  contacts is consistent with the published X-ray structure for the wild-type product form of HDV,<sup>6</sup> which reveals five possible innersphere contacts ( $\text{O}^- \cdots \text{Mg}^{2+}$  distance  $\leq 2.8\text{ \AA}$ )<sup>15</sup> between  $\text{Mg}^{2+}$  and  $-\text{PO}_2^-$  and two contacts with  $\text{N}_7$  and  $\text{O}_6$  atoms on a guanosine residue (see Supporting Information for details). It is also consistent with absorbance-detected  $\text{Mg}^{2+}$  titrations in solution on the cleaved form of the ribozyme that showed a change in absorbance over similar range of  $10\text{--}100\text{ mM Mg}^{2+}$ .<sup>16</sup> Unfortunately, it is problematic to make direct comparison between the binding data in solution and in the crystal given herein since  $\text{Na}^+$  concentrations in the solution experiments were 20-fold higher. Similarly, the RNAs used in the current study differ slightly in sequence from those in previous studies, though it is unlikely that such sequence differences would lead to significant changes in the overall HDV structure or in the number of metal ions bound.

The close agreement in the predicted number of metal-bound phosphates between Raman, X-ray, and other solution studies, however, suggests characteristic features of the Raman signal itself that allow it to be used as a tool to study metal ion binding. Specifically, while the metal-induced attenuation and upshift in the Raman signal for  $-\text{PO}_2^-$  represents the combined signal of  $\text{Mg}^{2+}$ -phosphate interactions from all  $-\text{PO}_2^-$  positions in the HDV molecule, it is also true that the relative contribution of individual  $-\text{PO}_2^-$  positions to metal-induced changes in the Raman signal will reflect the extent to which they are bound by  $\text{Mg}^{2+}$ . Within a complex folded RNA, the relative occupancy of  $\text{Mg}^{2+}$  at  $-\text{PO}_2^-$  positions involved in specific metal ion coordination is expected to be significantly larger than that predicted for nonspecific interactions with  $-\text{PO}_2^-$  positions in other regions of the molecule. The crystallographic studies noted above show that HDV is no exception. Thus, the observation that metal-induced changes in the

Raman signal for  $-\text{PO}_2^-$  in HDV is both saturable (Figure S3) and predicts the same number of metal ions identified by an independent method suggests that the contribution of nonspecific metal interactions to changes in the  $-\text{PO}_2^-$  Raman signal of HDV is likely to be small relative to those predicted to be involved in direct innersphere coordination. The ratio of the attenuated  $-\text{PO}_2^-$  Raman signal in the presence of  $\text{Mg}^{2+}$  to that of the parent spectrum of  $-\text{PO}_2^-$  in the absence of  $\text{Mg}^{2+}$ , therefore, appears to provide an accurate estimate of the number of metal ions involved in direct innersphere interactions.

In summary, we have shown that Raman crystallography can provide a powerful approach for studying metal ion interactions in RNA that can complement traditional but less direct crystallographic and biochemical methods. This approach permits both qualitative and semiquantitative dissection of metal ion binding and should prove useful in the analysis of other functional RNA and RNA-protein complexes. Raman experiments also provide the potential to detect site-specific effects using isotope and chemical substitutions,<sup>17</sup> indicating broad potential of this approach.

**Acknowledgment.** We thank Drs. V. Anderson and M. Harris for discussions on dimethyl phosphate.

**Supporting Information Available:** Raman spectrum of aqueous  $[\text{Mg}(\text{H}_2\text{O})_6]^{2+}$ , quantum mechanical calculations, interaction between magnesium hydrate and dimethyl phosphate in aqueous solution, and  $\text{Mg}^{2+}$  binding sites in the crystal structure of HDV. This material is available free of charge via the Internet at <http://pubs.acs.org>.

## References

- (1) Feig, A. L.; Uhlenbeck, O. C. *The Role of Metal Ions in RNA Biochemistry*. In *The RNA World*, 2nd ed.; Cold Spring Harbor Laboratory Press: Plainview, NY 1999; p 287.
- (2) (a) DeRose, V. J. *Curr. Opin. Struct. Biol.* **2003**, *13*, 317. (b) Sigel, R. K.; Pyle, A. M. *Chem. Rev.* **2007**, *107*, 97.
- (3) (a) Kieft, J. S.; Tinoco, I., Jr. *Structure* **1997**, *5*, 317. (b) Maderia, M.; Horton, T. E.; DeRose, V. J. *Biochemistry* **2000**, *39*, 8193.
- (4) (a) Hougland, J. L.; Kravchuk, A. V.; Herschlag, D.; Piccirilli, J. A. *PLoS Biol.* **2005**, *3*, 1536. (b) Maderia, M.; Hunsicker, L. M.; DeRose, V. J. *Biochemistry* **2000**, *39*, 12113.
- (5) Gong, B.; Chen, J. H.; Chase, E.; Chadalavada, D. M.; Yajima, R.; Golden, B. L.; Bevilacqua, P. C.; Carey, P. R. *J. Am. Chem. Soc.* **2007**, *129*, 13335.
- (6) Ferre-D'Amare, A. R.; Zhou, K.; Doudna, J. A. *Nature* **1998**, *395*, 567.
- (7) (a) Perrotta, A. T.; Shih, I.; Been, M. D. *Science* **1999**, *286*, 123. (b) Nakano, S.; Chadalavada, D. M.; Bevilacqua, P. C. *Science* **2000**, *287*, 1493. (c) Ke, A.; Zhou, K.; Ding, F.; Cate, J. H.; Doudna, J. A. *Nature* **2004**, *429*, 201. (d) Das, S. R.; Piccirilli, J. A. *Nat. Chem. Biol.* **2005**, *1*, 45. (e) Nakano, S.; Bevilacqua, P. C. *Biochemistry* **2007**, *46*, 3001.
- (8) Lai, M. M. *Annu. Rev. Biochem.* **1995**, *64*, 259.
- (9) The HDV crystals we use contain the  $2'\text{-OCH}_3$  substitution at the U-1 position of the inhibitor strand and are surrounded by cacodylate buffer at pH 6.0.
- (10) Pye, C. C.; Rudolph, W. W. *J. Phys. Chem. A* **1998**, *102*, 9933.
- (11) "No  $\text{Mg}^{2+}$ " conditions are achieved by soaking crystals in  $50\text{ mM EDTA}$ ,  $\sim 5$  times during 20 h.
- (12) (a) Carey, P. R. *Biochemical Applications of Raman and Resonance Raman Spectroscopies*; Academic Press: New York, 1982; Chapter 5. (b) Guan, Y.; Wurrey, C. J.; Thomas, G. J., Jr. *Biophys. J.* **1994**, *66*, 225.
- (13) Anderson, V. E.; Christian, E. L.; Harris, M. E. Private communication.
- (14) Peleg, M. *J. Phys. Chem.* **1972**, *76*, 1019.
- (15) Juneau, K.; Podell, E.; Harrington, D.; Cech, T. R. *Structure* **2001**, *9*, 221.
- (16) Nakano, S.; Proctor, D. J.; Bevilacqua, P. C. *Biochemistry* **2001**, *40*, 12022.
- (17) Carey, P. R. *Chem. Rev.* **2006**, *106*, 3034.

JA801861S